

Dynamic tracking of flow boundaries in rivers with respect to discharge

Localisation dynamique des limites d'écoulement en rivières par rapport au débit

MOURAD HENICHE, *Main address: Research associate, corresponding author, Tel (1418) 6542691, Fax (1418) 6542600, E-mail address: mourad_heniche@inrs-eau.quebec.ca, INRS-Eau, 2800 rue Einstein, C.P. 7500, Sainte Foy (Qc) G1V 4C7, Canada**

YVES SECRETAN, *Professor, AIRH member, INRS-Eau, 2800 rue Einstein, C.P. 7500, Sainte Foy (Qc) G1V 4C7*

PAUL BOUDREAU, *Research engineer, INRS-Eau, 2800 rue Einstein, C.P. 7500, Sainte Foy (Qc) G1V 4C7*

MICHEL LECLERC, *Professor, AIRH member, Chairman of the Eco-Hydraulics section, INRS-Eau, 2800 rue Einstein, C.P. 7500, Sainte Foy (Qc) G1V 4C7*

ABSTRACT

A new Eulerian approach is proposed to track the dynamic position of flow boundaries in rivers with respect to flow discharge or tides. Associated to a two dimensional (2D) transient horizontal hydrodynamic model, it allows to define the configuration of watercourses in a broad hydrological register varying from dry conditions to severe flooding. The finite element method is used to develop the numerical prediction tool. It is employed to estimate not only the classical flow variables such as water surface level and velocity field, but also the position of the shorelines. In this paper, the strategy followed for building this «drying-wetting» model consists in letting the water surface move freely, everywhere in the domain including the dry zones, allowing it to plunge under the ground. Two practical applications on rivers of Québec (Canada) are presented. The first one deals with steady state situations on St. Marguerite River. The second one deals with the reconstitution of flood propagation on Chicoutimi River according to the extreme flooding events of July 96 in the Saguenay region.

RÉSUMÉ

Une nouvelle approche Eulérienne est proposée pour le suivi de la dynamique des rives en milieu fluvial en fonction du débit ou de la marée. Associée à un modèle hydrodynamique transitoire horizontal à deux dimensions (2D), elle permet de déterminer la configuration des cours d'eau dans une large gamme hydrologique allant d'un débit d'étiage jusqu'à celui d'une crue affectant la plaine inondable. L'outil numérique développé repose sur la méthode des éléments finis. Il permet non seulement d'estimer les variables classiques de l'écoulement, à savoir l'élévation du plan d'eau et le champ de vitesse mais également la position des rives. Dans ce papier, il est question de la démarche adoptée pour la mise en oeuvre de ce modèle hydrodynamique dit «couvrant-découvrant» où l'hypothèse de base consiste à laisser libre partout dans le domaine incluant les zones sèches le mouvement du plan d'eau qui peut ainsi plonger sous le fond. Deux applications pratiques sur des rivières de la province du Québec (Canada) sont présentées. La première est consacrée à des scénarios d'écoulements en conditions stationnaires sur la rivière Sainte-Marguerite. Le second traite de la reconstitution de la propagation de l'onde de crue sur la rivière Chicoutimi survenue lors du déluge du Saguenay en juillet de 96.

1. Introduction

Studies of water system management reveal the opportunity to employ an efficient numerical tool in modeling two dimensional horizontal hydrodynamics of rivers, at the reach scale, especially for extreme events in order to track the dynamic position of the shorelines. In this paper, it is assumed that the shoreline represents the contour line of zero depth; it is also a flow boundary. Under the strong variation of the discharge or the tide, the configuration of flow river can change considerably and the displacement of the flow boundaries can be very important. Indeed, such a simulation tool is undoubtedly an appreciable support in decision help for policy-maker in the design of a cartographic survey of flooding area. It can also provide assistance to dam managers in predicting the effects of water level control upstream or of the dropped discharge downstream. From an environmental view point, the dynamic location of the shorelines is an important factor for biologists whose research focuses on fish habitat and aquatic plants. These examples show the interest to develop a drying-wetting model for fluvial hydrodynamics. The finite element method (FEM) has proved to be particularly adapted for modeling the terrain data complexity as encountered in natural

conditions. Therefore, the INRS-Eau research center of Université du Québec is engaged since 1992 in the development of a 2D drying-wetting hydrodynamic finite element model for rivers and estuaries called HYDROSIM, which takes into account the dynamic position of the shorelines during the computation. This operation is not trivial, and to achieve it, a daring approach was performed. Basically, no assumption is made on the free surface position which is free to plunge under the bed topography, generating non physical negative water depth. Thus, the regions with negative and positive water depth are considered respectively dry or wet areas. The shoreline is then given by the contour line corresponding to zero water depth [Heniche *et al.*, 2000]. This method has been used with success in many projects, involving rivers located in the province of Québec (Canada), where significant displacements of the shorelines were observed, such as in the reconstitution of the flood disaster of July 1996 in the Saguenay region [INRS-Eau, 1997], the damages estimation to residences due to submersion in Chicoutimi and Aux Sables Rivers [Leclerc *et al.*, 1997] and the flow sensitivity analysis on the Montmorency River [Leclerc *et al.*, 2000] among others.

The outline of the paper is as follows: the next section describes

**Present address: Mourad Heniche, Research associate, URPEI, Ecole Polytechnique Montreal, Montreal, QC, Canada, H3C 3A7, Phone: (514) 3404711 ext. 5778, Fax: (514) 3404105, E-mail: mourad.heniche@polymtl.ca*

Revision received February 6, 2001. Open for discussion till February 28, 2003.

the basic approach in predicting the position of the shorelines of a river. Section 3 deals with the mathematical model of the 2D steady shallow water equations. In Section 4 the finite element discretization of the drying-wetting model is presented. Finally, two numerical applications on St.-Marguerite River and Chicoutimi River are described in Section 5.

2. Tracking shoreline approach

There exist two broad classes of methods for modeling the moving boundaries: Eulerian and Lagrangian. The main difference can be summarized briefly by the state of the computational domain. The Eulerian method is characterized by a fixed computational domain. If the computational domain evolves with the position of the moving boundary, the method used is Lagrangian. Leclerc *et al.* (1990) reviewed the several approaches available. The choice of the Eulerian or the Lagrangian method is then influenced by the physical phenomenon. In tracking the shorelines of rivers, it appears that the Eulerian method is more appropriate than the Lagrangian method which is harder to program and can be much more complicated to apply, especially in complex topography. For instance, in hydrodynamics modeling, the shoreline can be seen as a moving boundary between dry and wet regions. It depends on the water depth value H achieved by the differentiation between the water surface level h and the terrain topography z_b , which must be equal to zero ($H=h-z_b=0$, Fig. 1).

The first question which rises to mind is how to treat the water surface level in the dry area in a modeling process. The simplest method is to consider the free surface as a moving plane which covers the whole computational domain and let it free to plunge below the ground. This hypothesis on water level position generates positive and negative water depths. The sign convention (Fig. 1) adopted gives positive depth for wet areas and negative depth for dry ones. The second question is related to the implementation of this approach. Three conditions are required. Obviously, in the wet area, one has to respect the classical principles of mass and momentum conservation governing the free surface flow (zone A, Fig. 2). On the other side, in the dry area, one has to respect the

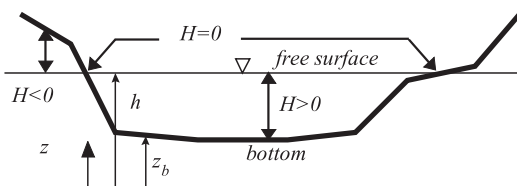
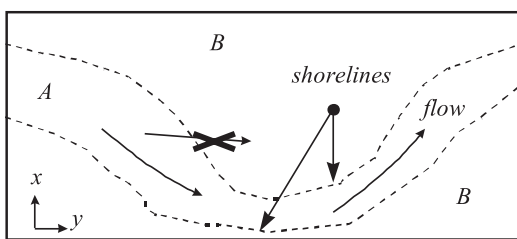


Fig. 1. Free surface configuration.



A : wet area B: dry area

Fig. 2. Computational domain with drying-wetting areas.

no flow condition (zone B, Fig. 2). Finally, the third condition is the no mass transfer criterion across the interface between the wet and the dry area, to make the shoreline an impermeable moving boundary.

3. Two dimensional hydrodynamic model

Transient shallow water equations

In an attempt to locate the shorelines over the computational domain, the water surface elevation and the velocity field, the two dimensional vertically averaged transient shallow water equations [Jansen *et al.*, 1979] governing the momentum balance and mass balance are solved. It must be remembered that the fundamental hypothesis of the model supposes a small depth in relation to the horizontal size, a well mixed water column with a constant density, a hydrostatic pressure distribution and a constant horizontal velocity profile in the vertical direction. In the flux formulation, with water level scalar h and specific discharge vector $q(q_x, q_y)$ as the state variables, the set of three partial differential equations, including Coriolis force and wind stresses, are written in Eulerian form with t as time variable and in Cartesian coordinates $x(x, y)$ as follows:

$$\frac{\partial p H}{\partial t} + \text{div} q = 0 \quad (1)$$

$$\frac{\partial p q}{\partial t} + \text{grad}(H q \otimes q) + c^2 \text{grad} h - \frac{1}{\rho} [\text{div}(H \bar{\tau}) - \tau^b + p \tau^s] + f_c = 0 \quad (2)$$

where (1) represents the continuity equation and (2) represents the momentum equations, in x and y directions respectively, written in vectorial form. The porosity p is introduced to control mass and momentum transfer between dry and wet areas in the unsteady case. It is equal to 1 in the wet area and 0 in the dry one. The celerity of shallow water waves is noted by c ($c = \sqrt{gH}$) which results from the square root of the product between the gravitational acceleration g and the water depth H . For the determination of the Reynolds stresses components of the $\bar{\tau}$ tensor, an algebraic turbulence model depending on the so called mixing length is employed to estimate the eddy viscosity [Rodi, 1982].

The bottom friction τ_i^b obeys the Chézy-Manning law, thus:

$$\frac{1}{\rho} \tau_i^b = C_b^f |q| q_i = \frac{g n^2 |q| q_i}{H^{7/3}} \quad i \equiv j = 1, 2 \equiv x, y \quad (3)$$

where C_b^f is the bed friction coefficient and n is the dynamic Manning roughness number. They play an important role in the drying-wetting model discussed next. The wind stresses τ^s is independent from the hydrodynamic components. Thus, to annihilate its action in the dry area, it is weighted by the porosity. More details about the governing equations are available in a previous author's paper (Heniche *et al.*, 2000)

Remark: Although the riverbed is assumed to be fixed, it is quite easy to verify in equation (1) that

$$\frac{\partial p H}{\partial t} \neq \frac{\partial p h}{\partial t}$$

in the transition zone which becomes dry or wet.

Dirichlet boundary conditions

The computational domain Ω is bounded by two kinds of boundaries: the closed one Γ_c and the opened one Γ_o . The available Dirichlet boundary conditions (BCs) are given by the following. Impermeability condition is achieved since the normal component q_n to Γ_c is set to zero:

$$q_n = 0 \text{ on } \Gamma_c$$

On the inflow boundary Γ_o , one can impose either water level or its equivalent flow rate:

$$h = \bar{h} \text{ or } q_n = \bar{q}_n \text{ on } \Gamma_o$$

On the outflow boundaries Γ_o , the water level h , which can be time dependent, is imposed:

$$h = \bar{h} \text{ on } \Gamma_o$$

Initial solution

The choice of the initial solution is crucial especially for the first simulation. For instance, taking into account that in hydrodynamics the driving force of the flow is the free surface gradient, numerically it is often suitable to employ the following initial solution:

$$h = h(x, y) \\ q_x = q_y = 0$$

where the elevation function $h(x, y)$ must be physically acceptable as soon as it generates a correct flow. In practice, it is a matter of starting with the simplest hydrostatic situation which satisfy (1), (2) and (3). The initial position of the free surface is imposed as the mean value between inflow and outflow boundaries when the elevation difference between Γ_o^{in} and Γ_o^{out} does not exceed approximately 0.5÷1.0 m. However, this approximation is heuristic and is strongly influenced by the characteristics of the flow and the solver used.

4. Finite element drying-wetting model

Properties of governing equations

One of the most important properties of the momentum equation (2), when neglecting Coriolis force and wind stress, is their parity with respect to the depth H . It means that the shallow water equations may reproduce the same problem with negative or positive water depth H . Taking advantage of this mathematical particularity, and in compliance with the initial hypothesis about the posi-

tion of the free surface, the basic idea is to drive the flow from the dry area ($H < 0$) to the wet one ($H > 0$). Considering the characteristics of flows in rivers, it is well known in hydrodynamics that the major contributions in equation of motion (2) are given by the global equilibrium between the free surface level and the friction terms. In order to respect the principles of mass and momentum conservation in the wet area, the original mathematical model is adapted with the aim of freezing the flow within the dry area. To achieve this, the action of the friction operator is significantly increased through a modification of the Manning coefficient n based on the depth value H . In the wet area, the Manning coefficient is set in accordance with local flow resistance properties:

$$n_{H \geq 0} = n \quad (4)$$

However, in the dry area, n varies linearly as a function of H as follows:

$$n_{H < 0} = n(1 + \beta|H|) \quad (5)$$

For small depth, equation (5) generates a low Manning dry friction but C_b^f become large because the depth appears in $1/H^{7/3}$ in its expression. Numerical experience demonstrates that accuracy is higher at greater β values, but the cost of calculation is much greater: a damping coefficient β typically equal to 100.0 seems optimum for fluvial studies. Programming the proposed approach in a finite element code is quite easy and does not require any diagnostic test (if conditions on the dry-wet state of nodes and elements), thus providing a higher numerical efficiency.

Matrix formulation

The finite element method is employed to discretize the governing equations over the multi-linear triangular 6-node finite element *T6L*, which is a combination of four 3-node triangular elements, is used for the discretization of the computational domain. To satisfy compatibility conditions, the approximation of the water level is linear on the main triangle. On the other side, the approximation of the specific discharge is linear on each sub triangle. Numerical dissipation driven by the Peclet number is added to smooth the solution when convection dominates the flow. This element has satisfied all tests of stability and precision but its major draw-back, as all stable finite elements in fluids with continuous pressure approximation, is that it does not satisfy local mass conservation (Galland & al., 1991). Local mesh refinement is the standard way to reduce error on mass conservation to an acceptable level of accuracy. In the construction of finite element matrix the depth is kept in absolute value to reduce advection in transition zone. In addition, depth truncature technique is employed to deal with small depth to avoid singularity of the system. As we have two kind of equations, time dependent in the wet area and steady state in the dry area, we have for stability consideration employed the implicit Euler scheme. The expression of the residual $\{R\}$ is the following:

$$\{R\} = \{R\}_D + \{R\}_T + \{R\}_W = \{0\} \quad (6)$$

with

$$\{\mathbf{R}\}_D = ([\mathbf{K}(\mathbf{U})]\{\mathbf{U}\} - \{\mathbf{F}\})_{t+\Delta t} = \{0\}$$

$$\{\mathbf{R}\}_T = [\mathbf{M}](\{p\mathbf{U}\})_{t+\Delta t} - \{p\mathbf{U}\}_t + \Delta t([\mathbf{K}(\mathbf{U})]\{\mathbf{U}\} - \{\mathbf{F}\})_{t+\Delta t} = \{0\}$$

$$\{\mathbf{R}\}_W = [\mathbf{M}](\{\mathbf{U}\})_{t+\Delta t} - \{\mathbf{U}\}_t + \Delta t([\mathbf{K}(\mathbf{U})]\{\mathbf{U}\} - \{\mathbf{F}\})_{t+\Delta t} = \{0\}$$

where the subscripts D, T and W are related to dry, transition and wet zones respectively. The [M] matrix comes from time derivative discretization, [K] is the stiffness matrix, the {F} vector contains wind stresses and boundary conditions and Δt denotes time step. The algebraic nonlinear set of equations (6) is solved to find the solution {U} with an inexact-Newton-GMRES algorithm using efficient dynamic fill level Incomplete Lower-Upper (ILU) factorization of the Jacobian matrix as left preconditioning, and block numbering of the unknowns [Heniche *et al.*, 2001]. The choice of this solver satisfies two important requirements. First, the main advantage of this iterative solver is that it does not need to store a large matrix, compared to a more direct method. Second, it is well known that the GMRES method proposes a strong criterion known as the minimization of the residual, objective of the FEM solution procedure, which can support the parametrical shock arising from the strong variation of the friction term especially on the transition elements.

Limitations

We have used this model to study in a satisfactory manner a wide range of fluvial applications most of them in steady state case. When the general flow is tangential to the flow boundaries the model works well. Nevertheless, two impediments, beyond the scope of this paper, are pointed out: small depth and resurgence. First, shallow water models are quite sensitive to small depth, a singularity in the momentum equations particularly in flux formulation. The standard way to overcome the problem but still unresolved is to employ depth truncature technique. Since it leads to difficulties of convergence from both explicit and implicit schemes and/or to poor results in the vicinity of front surge. The friction law is probably the main cause as C_b^f goes to infinity for small depth which degrades the conditioning of the discrete system to solve (Fennema and Chaudhry, 1990; Zhang & *al.*, 1992; Khan, 2000). Second, resurgence phenomenon is closely related to the drying-wetting model proposed. It occurs most of the time for high speed flows through channel contraction or around a pier for example. Free surface is of high gradient streams and induces a non negligible normal flow component across the boundary of the contraction or the pier even if the flow is negligible inside the dry area. In steady state case the problem is easily manageable as it consists to remove from mesh all the elements which contribute to resurgence. But in unsteady case the problem is less manageable.

5. Practical applications

The presented approach was implanted in HYDROSIM, a finite element FORTRAN-C/C++ code devoted to flow analysis and currently employed at the INRS-Eau research center for fluvial studies. Two of them are presented next where the first one is a steady state case and the second one is an unsteady case.

St.-Marguerite River: steady state case

The present model was applied on the St.-Marguerite River, on a reach 1.15 km long and 50.0 m wide (mean width) (Fig. 3). This natural field is characterized by a curved geometry, a complex bed topography and a variable friction coefficient. The bottle neck of a real life hydrodynamic study is the availability of the terrain data because the hydrodynamic model requires at least the bed topography and the friction Manning coefficient. The terrain data used was initially employed for a research project on fish habitats by Lafleur (1997). For instance, an overall view of the topography data along the longitudinal profile is shown in Fig. 5. On the computational domain, the following statistic on the data was observed; the minimum bed elevation is 108.0 m and the maximum is 114.0 m; as well, the Manning coefficient varies from 0.015 for smooth bed to 0.042 for the rough one.

Modeling approach

The St.-Marguerite River reach of this study is not affected by tide. During the field campaign, the discharges were measured at control section 3 (Fig. 3) and the flow was assumed in a quasi steady state condition. Thus all the scenarios simulated are in steady state conditions. Two carefully designed meshes, a coarse one and a refined one, were employed. The coarse mesh has 9487 *T6L* elements, 4.0 m mean size, and 19566 nodes, which corresponds to 48698 unknowns. The refined (locally) mesh, presented in Fig. 4, has 11279 *T6L* elements, 2.0÷4.0 m mean size and 23216 nodes, which corresponds to 69648 unknowns. The refinement were located in the zone where the most important errors on mass conservation were encountered, near the inflow and the outflow boundaries and in the bend between section 2 and section 3 (Fig. 3). To improve the present method, the two meshes cover all the terrain data to predict stream bed and flood plain elevations. The global strategy used in the simulation procedure can be summarized by the following. No special mention is retained for solution procedure which is quasi automatic. The major effort is made on the tuning of numerical dissipation and on the post processing in checking the quality of the solution in terms of residual norms ($<5 \times 10^{-4}$), mass conservation ($<5\%$) and flow discharge value.

Results

A wide hydrological register ($Q=7.4; 19.2; 50.0$ and $100.0 \text{ m}^3/\text{s}$) was simulated in order to improve relevance, accuracy and robustness of the computational algorithm. The refined mesh was used to simulate 7.4 and $19.2 \text{ m}^3/\text{s}$ events and the coarse mesh for the two others. As BCs, water level was prescribed on the open

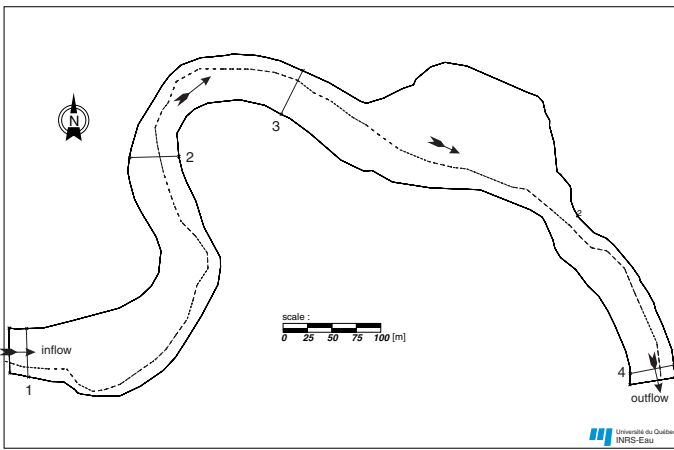


Fig. 3. St.-Marguerite River reach : flow direction, longitudinal profile and cross sections.

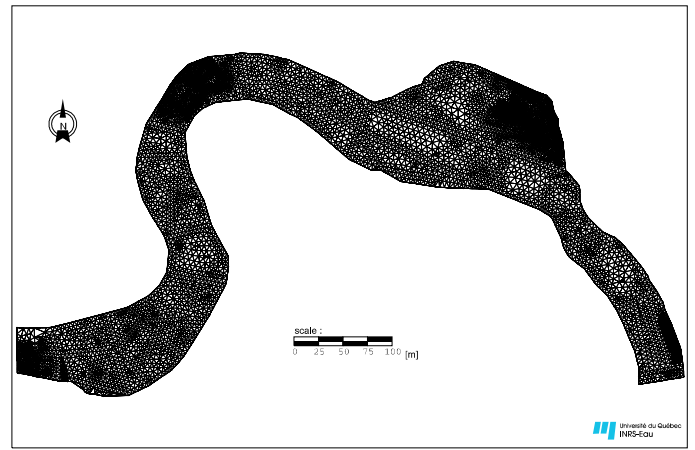


Fig. 4. St.-Marguerite River reach: refined mesh (11279 elements, 23216 nodes).

boundaries according to Table 1. Moreover, on the inflow boundary the flow direction ($q_r=0$) was also prescribed. Static conditions ($q_x=q_y=0, h=constant$) were used as initial solution. The time computation of the initialization procedure varies between 3 and 4 hours, on P.C. Pentium with a 133 MHz processor and 64 MB RAM memory, depending on mesh and event. After that, each tuning procedure is approximately twice as fast.

Table 1. Discharge-water level on inflow and outflow boundaries.

$Q (m^3/s)$	$h (m)$ at inflow	$h (m)$ at outflow
7.4	112.03	111.10
19.2	112.23	111.43
50.0	112.70	111.81
100.0	113.15	112.14

Different views of the computed positions of the free surface are presented in order to estimate the relevance of the proposed approach. For instance, the variations of the longitudinal profiles of the free surface along the stream bed for the different events are shown in Fig. 5. The transversal profiles at control sections, where the origin is on the left bank of the river, in Fig. 6, show

that the water level plunges under the bed topography in accordance with the simulated discharge. The position of the shorelines on a horizontal plane for the four events are shown on Fig. 7. They reveal a drastic change in the horizontal configuration of the river section. One can appreciate the progressive disappearance of all the islands from the lowest to the maximum discharge. At maximum discharge the flow covers practically the entire domain. For high flows, the discontinuities of the shorelines are observed where mesh spatial coverage is limited because of a lack of terrain data.

Validation

The operation of validation of the numerical model was made with the event of $Q=19.2 m^3/s$ where the refined mesh was employed. The 7 water level measurement points are located left bank along the stream bed (Fig. 8). For the velocities, we have 17 measurement points located on control section 3.

Table 2 presents the measured and computed water level values at the measurement locations. One can see that the maximum difference does not exceed 8 cm and the correlation factor is 0.99. In Table 3, we have the same exercise on the velocities where the maximum differences are located near the shoreline. However, in the middle part of the bed flow, the results are in good agreement

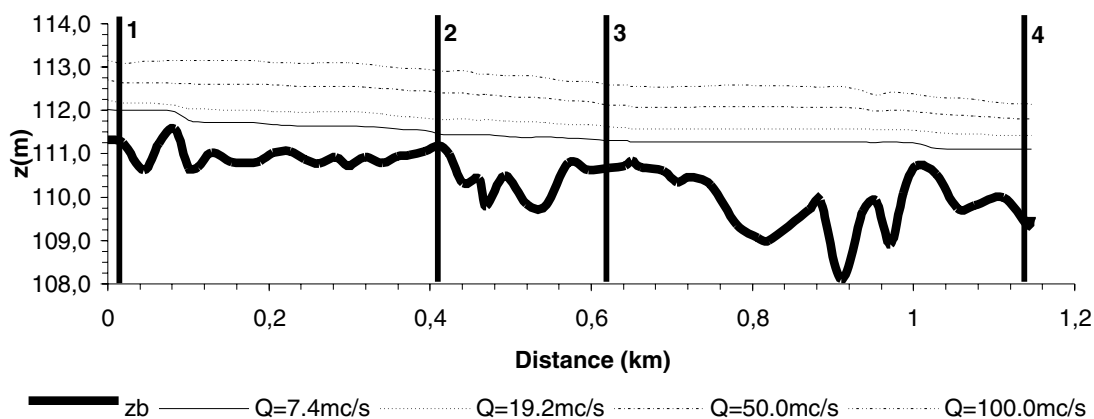


Fig. 5. St.-Marguerite elevation profile along the stream bed.

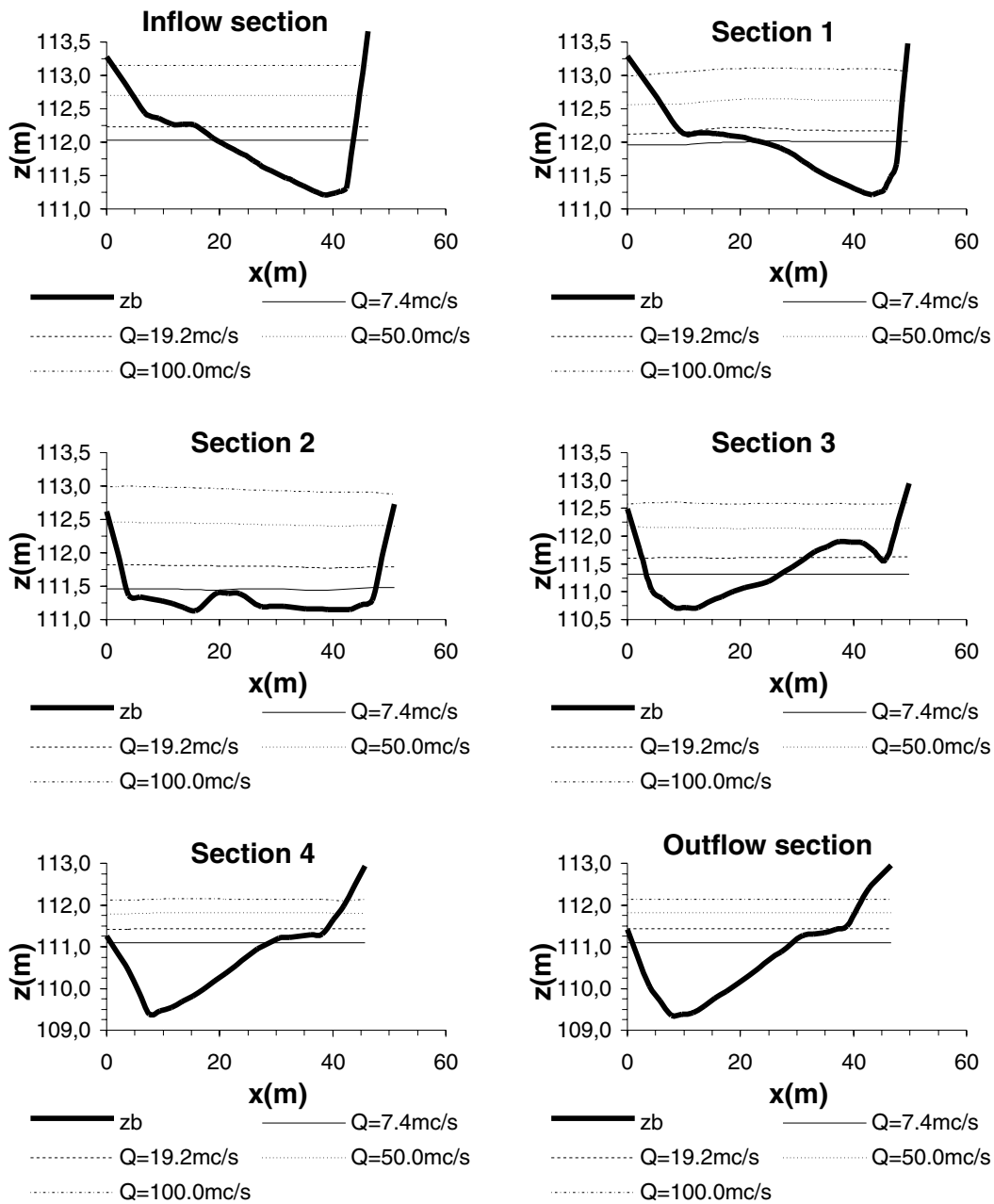


Fig. 6. Water level at control sections.

with the experiment. Despite these differences, the velocity correlation factor reaches 0.95. The transversal profiles at control sections in Fig. 10 show that the velocities vanish as soon as the water depth is inferior to zero. Moreover, to achieve mass conserva-

tion in the stream bed, the transversal velocity distribution varies according to the wet area of the cross section.

Table 2. Water level validation for $Q = 19.2 \text{ m}^3/\text{s}$.

Location	Measured h_m (m)	Computed h_c (m)	Difference $h_c - h_m$ (m)	Location	Measured h_m (m)	Computed h_c (m)	Difference $h_c - h_m$ (m)
1	111.43	111.43	0.00	5	111.97	111.96	-0.01
2	111.62	111.54	-0.08	6	111.97	112.00	0.03
3	111.62	111.57	-0.05	7	112.18	112.18	0.00
4	111.79	111.81	0.02				

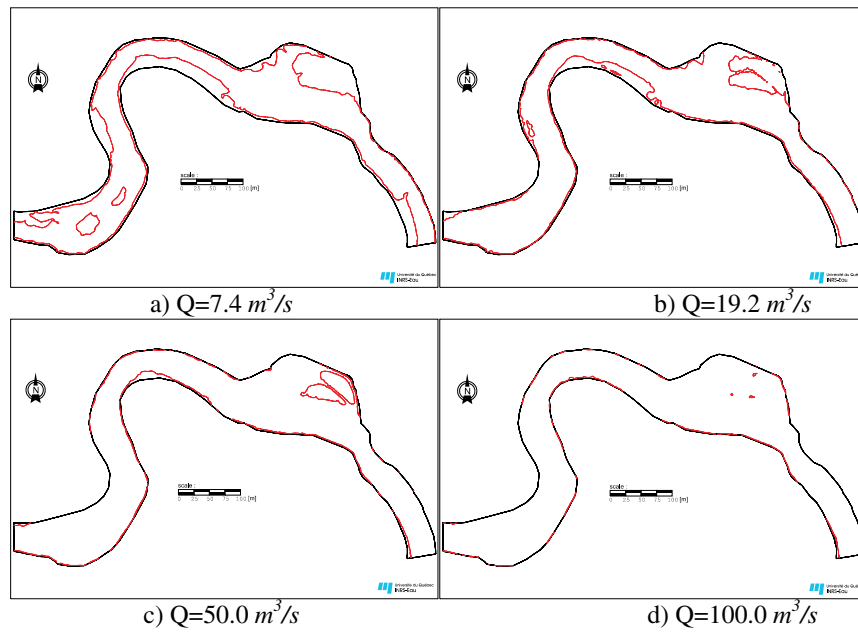


Fig. 7. Computed position of the shorelines.

Table 3. Velocity validation for $Q=19.2 \text{ m}^3/\text{s}$.

Location	Measured V_m (m/s)	Computed V_c (m/s)	Difference $V_c - V_m$ (m/s)	Location	Measured V_m (m/s)	Computed V_c (m/s)	Difference $V_c - V_m$ (m/s)
1	0.00	0.00	0.00	10	1.22	1.23	0.01
2	0.41	0.21	-0.20	11	1.22	1.22	0.00
3	0.77	0.54	-0.23	12	1.22	1.25	0.03
4	0.80	0.77	-0.03	13	1.17	1.22	0.05
5	0.77	0.90	0.13	14	1.06	1.06	0.00
6	0.92	1.07	0.15	15	0.83	0.81	-0.02
7	0.96	1.14	0.18	16	0.58	0.44	-0.14
8	1.06	1.13	0.07	17	0.00	0.25	0.25
9	1.16	1.25	0.09				

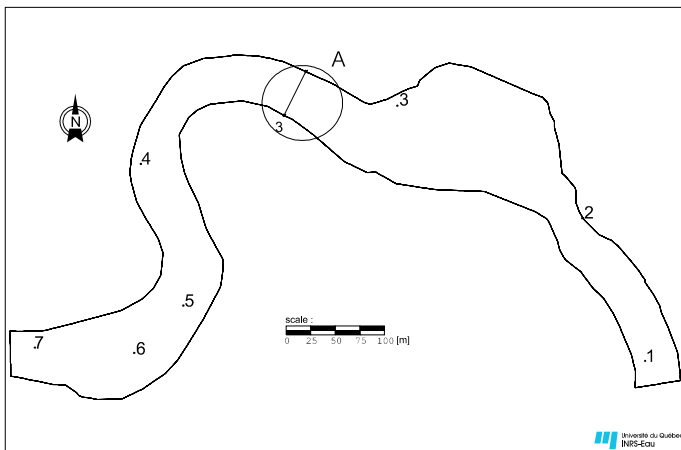


Fig. 8. St.-Marguerite River reach: location of water level measurement points.

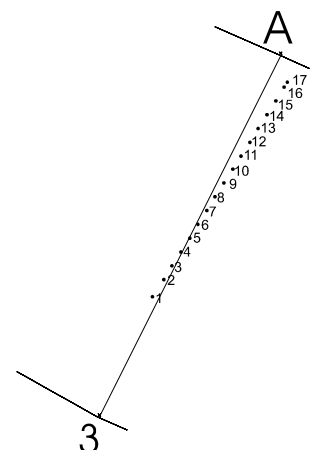


Fig. 9. St.-Marguerite River reach: distribution of velocity measurement points at control section 3.

Situation

The Saguenay region in the center of Québec province was strongly affected by a huge flood in July 1996 which is commonly known as «le déluge du Saguenay». For the comprehension of the reader, we recall briefly the events focusing only on the river reach of this issue. The site of interest is presented in Fig. 11, one can see the map of the Chicoutimi river reach which is discussed hereafter. During 72 hours, from July 18 to 20, it was recorded 250 mm average precipitation on the overall watershed and it resulted in an exceptional runoff. Even empty, Kénogami lake reservoir did not have the potential to catch the flood. As consequence, water level of Kénogami lake increased until it exceeded the crest of Portage-Des-Roches dam July 20. The discharge became out of control and increased dramatically on Chicoutimi river. The flows was so important that it caused severe inundations which contribute to circumvent left bank Chute Garneau dam and emptying its reservoir.

Chicoutimi River: transient case

Early after the torrential rains and the floods which occurred in the Saguenay region, the Québec government established the Scientific Commission on Dams Management (Commission Scientifique et Technique sur la Gestion des Barrages, CSTGB). Its mandate was to investigate the exceptional climatic and hydraulics events which caused huge damages in the region. We were committed by the CSTGB to reconstruct by numerical simulation the events in order to determine as best as possible the flood limits. The implementation of a two dimensional hydrodynamic model in a context of transfer of an exceptional flood wave in a real case is not a commonplace problem (Chow, 1959). To perform this analysis, it requires at least hydrologic and terrain data as well as a hydrodynamic model able to dynamically track river flow boundaries.

Terrain and hydraulics data

Between Portage-Des-Roches and Chute Garneau dams, this river reach nearly 17 km long could be divide in three parts: upstream,

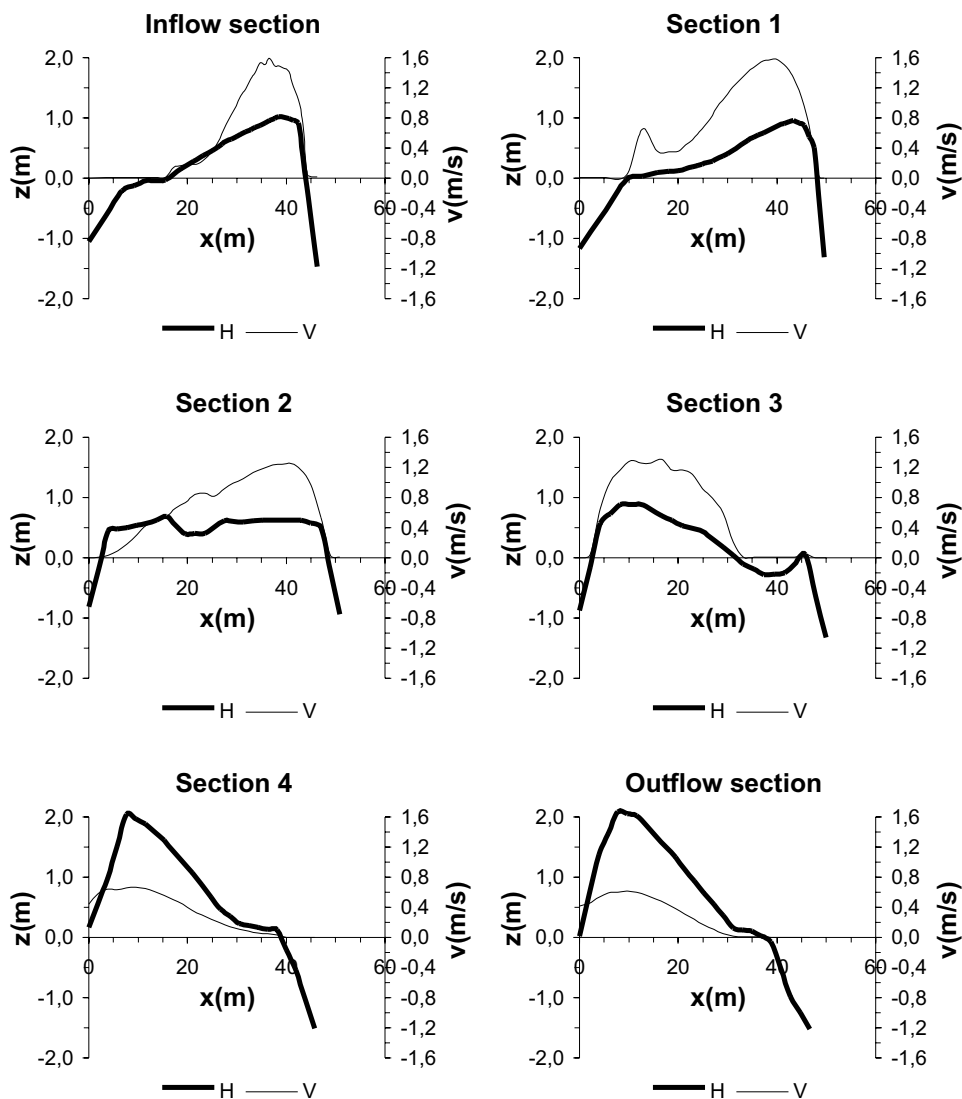


Fig. 10. Velocity distribution for $Q=19.2 \text{ m}^3/\text{s}$ at control sections.

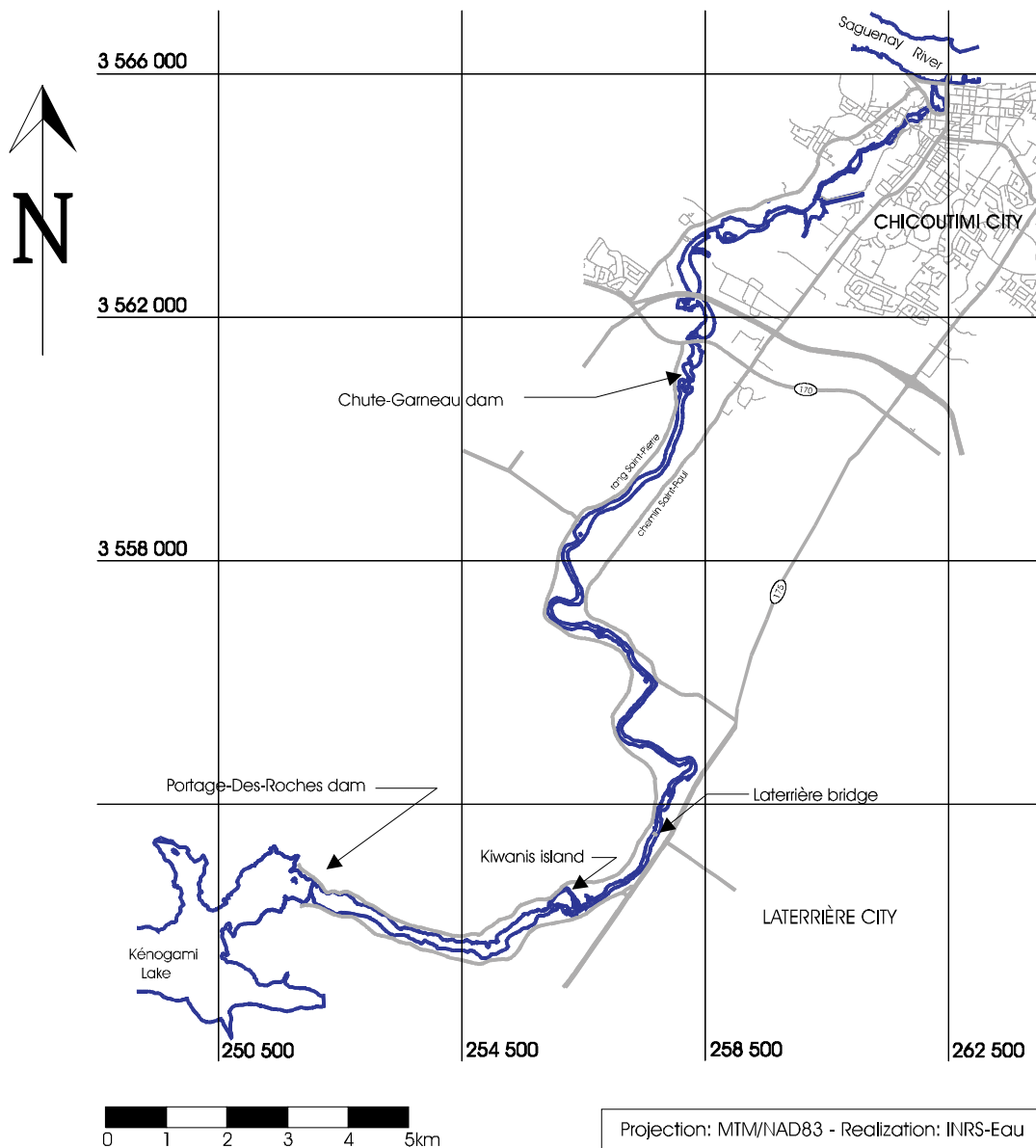


Fig. 11. Saguenay flood: site map between Portage-Des-Roches and Chute Garneau dams.

middle and downstream part. Upstream, between Portage-Des-Roches dam and Kiwanis island, the stream is irregular along 4 km with a 150 m average width and the river flows on bed rock with a 0.002 average slope. Middle, between Kiwanis island and Laterrière bridge, the stream is straight along 2.5 km and of highest bed slope about 0.003. Downstream, the stream is smooth with well developed meanders along 10.5 km of a 80 m average width and the river flows on alluvial deposits with a 0.001 average slope. The Numerical Terrain Model (NTM) employed was constructed with two data sets. In the flood plain, photogrammetry technique enables to generate data points with $\pm 75\text{cm}$ accuracy. In the riverbed, few transects data points obtained with total station were available. To reproduce meanders additional synthetic transects have been added using linear curvilinear interpolation with respect to normal bank. The NTM was realized with MODELEUR, a combination of GIS and finite element pre- and post processor (Secretan and Leclerc, 1998). To perform the hydrodynamic simulation the required boundary conditions are the discharge upstream and the water level downstream. The time

varying discharge were provided by the streamflow produced by CEQEAU, a hydrologic model (Morin & al., 1995), and presented in Fig. 12. During the extreme flood of July 1996, according to the streamflow, the $1100\text{ m}^3/\text{s}$ maximum discharge observed was approximately 4 times greater than the river overflow discharge in the range of $250\text{-}300\text{ m}^3/\text{s}$. If one consider that the wave flood travel this reach in 3 to 4 hours, so at maximum of the flood steady state conditions was established. Fig. 13. shows the water level signal which was imposed on the downstream limit of the hydrodynamic model. One notes more than 4,0m total variation in three main phases in accordance with streamflow: rapid rise (July 20), significant decrease of growth at maximum flow (July 21) and a rapid fall resulting from circumventing of Chute Garneau dam (July 21). It should be noted that the data of water level are an amalgam of direct observations recorded by Chute Garneau dam administrator (until the overflow phase), then of reconstitution according to testimonies of observers and photographic or video documents made up following the events.

Simulation procedure

The unsteady simulation was carried out going from 20h00 Friday July 19 to 24h00 Thursday July 25, 1996. The mesh used has 18243 nodes and 8722 finite elements which correspond to 54279 degrees of freedom and 41207 equations to solve. The boundary conditions used are those presented in Fig. 12 for discharge at inlet boundary and of Fig. 13 for water level at outlet boundary. The initialization procedure remained to reproduce the steady state conditions which prevailed in the beginning of the events. The discharge magnitude was $137 \text{ m}^3/\text{s}$ and water level downstream was 136.5 m the normal exploitation level of Chute Garneau reservoir. The strategy employed to compute the initial solution was based on the determination of an approximate water level plan and the fluxes set to zero. The transient simulation started July 19 at 20h00 with the initial state discussed previously. For numerical efficiency considerations (convergence, accuracy and computational costs), preliminary computations were conducted to select the appropriate flood routing time step. A 5 minutes time increment was found to be optimal. The simulation was conducted on a UNIX Silicon Graphic R4000 machine where approximately 60 hours CPU time permit to reproduce 24 hours real time. The computational time were inflated because of the well known GMRES stagnation occurred at different time steps (the analysis of the residual revealed that local non convergence appeared on few nodes located along the shoreline) without affecting the quality of the results. For obvious practical considerations, the results were stored at each hour which required 400 MB total space on hard disk.

Results

The results of the transient simulations are presented on Fig. 14, Fig. 15 and Fig. 16. Water rise and fall are presented on Fig. 14 where maximum water profile is displayed on each of the 8 graphs. First and second graphs show computed water surface July 19 and 20 each hour from 20h00 noon to 4h00 morning where beginning of water rise started July 19 at 0h00. Water rise is especially pronounced in the meanders region. As mentioned earlier, it is less wider than upstream that's why it is more sensitive to discharge variation. Moreover its effect upstream is mod-

erate by the Kiwanis island rapid flows. On the six others graphs the water surface profile is displayed at all 6 hours. Water rise continued all the day of July 20 at an average speed of 17 cm/h . Between midday and 18h00 on July 20, the water level rose of almost 2.0 m in six hours (35 cm/h) downstream of Kiwanis island whereas it rose only the half upstream during the same period. Water level was at maximum July 21 where we observe that, according to places, the level of the river increased from 3.5 to 4.5 m between the beginning of the events and the maximum of the flood. The third day flood July 22, water level was also at maximum and in addition we observe the emptying of Chute Garneau reservoir. It is the consequence of left bank circumventing flow, which unfortunately has no or few effect on water level upstream (M2 type backwater curve). The beginning of water fall at 2 cm/h average speed is observed July 23 until July 25 while the flow was already out of bank. To show the importance of the flood from a social view point, plan view of computed flow boundaries at different moments of the flood are displayed on Fig. 15. Flow boundaries in the more sensitive area are superposed on a digital image radar produced by the Canadian Center of remote sensing. One distinguish clearly the river stream and the inundate infrastructures such as residences, streets, roads and everything else of Laterrière City. Normal flow bank was used to calibrate the initial solution used to start the simulation of the flood propagation. Maximum levels simulated and observed, from marks and garbage forsaken on flood plain by water fall, are shown on Fig. 16. One observes a good correspondence between simulations and observations.

6. Conclusion

The scope of this paper has focused on numerical modeling study of dynamic tracking of flow boundaries according to discharge in open channels in both steady state and transient real cases. The prediction of the dry and wet zones of the river is based on free vertical displacement of water surface. No assumption is made on the water level position which should generate positive and negative water depth values. The determination of flow boundaries remain to display the zero depth contour line. The authors have improved this method in many fluvial studies. The selected examples show the ability of the proposed approach to work in com-

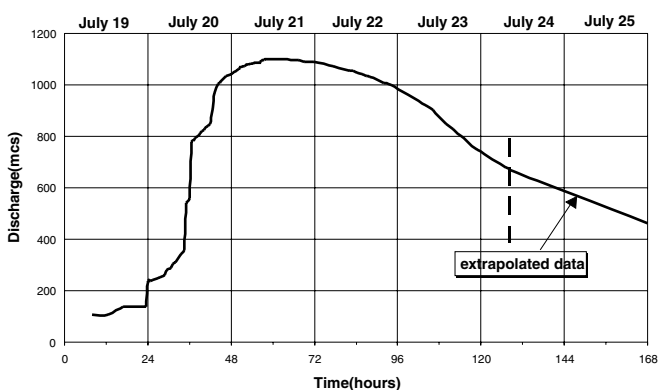


Fig. 12. Saguenay flood: streamflow at Portage-Des-Roches dam.

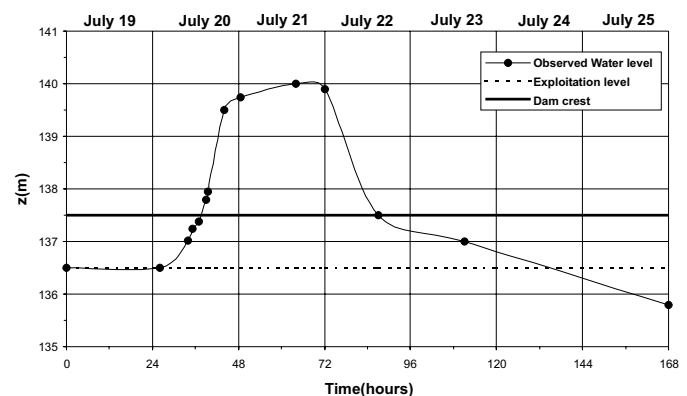


Fig. 13. Saguenay flood: water level at Chute Garneau dam.

plex topographic configurations and in wide range discharge. To make the model of more general use, further investigations in two ways should be useful namely small depth and resurgence.

Acknowledgements

The authors would like to acknowledge Ministry of Environment and Fauna of Québec and Commission Scientifique et Technique

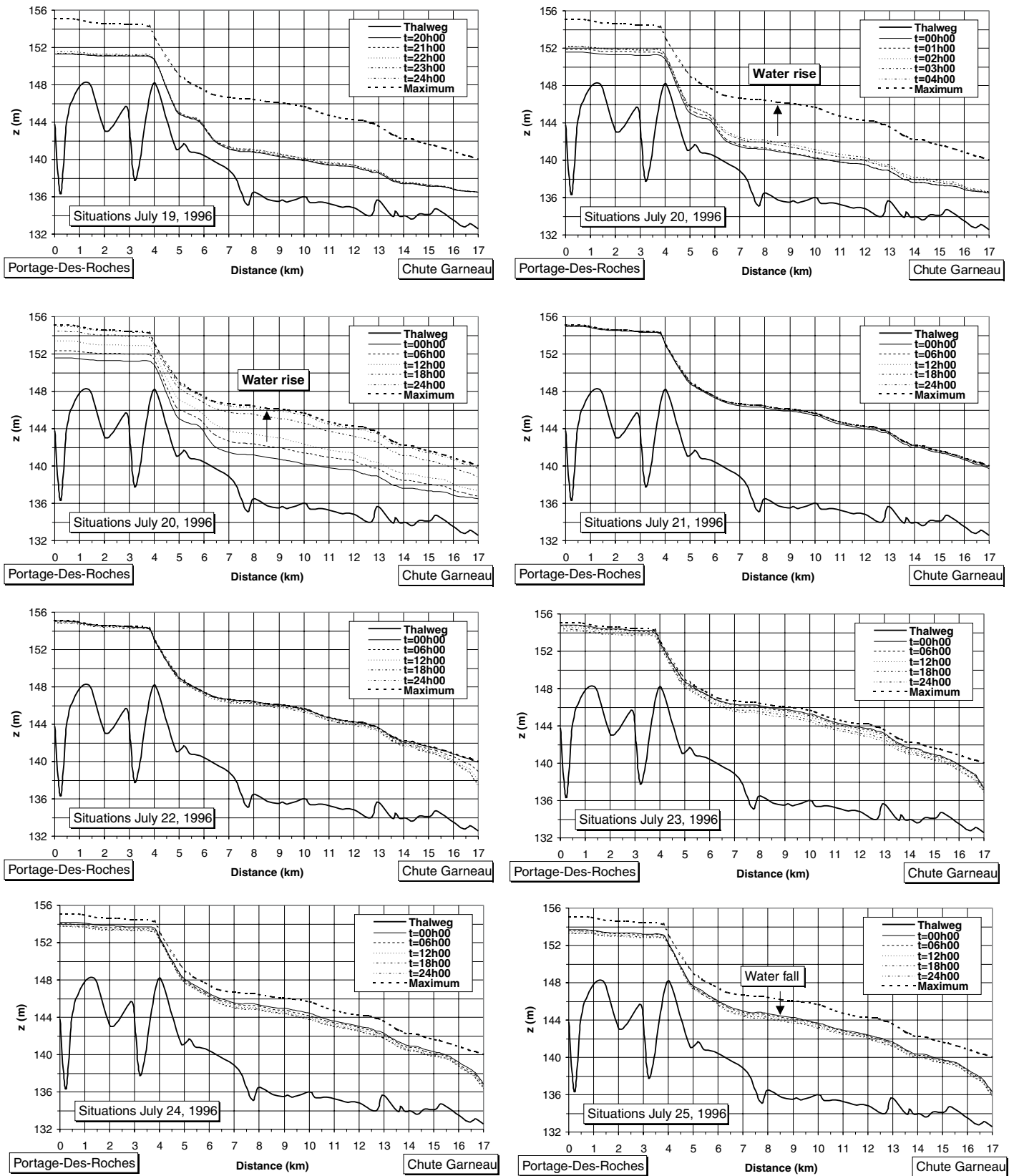


Fig. 14. Saguenay flood: simulated time varying water surface profile.

sur la Gestion des Barrages (CSTGB) for their financial assistance in the development of the numerical tools used in this study. They thank Environment Canada and Groupe Interdisciplinaire de Recherche en Éléments Finis (GIREF) for giving access to the hardware resources.

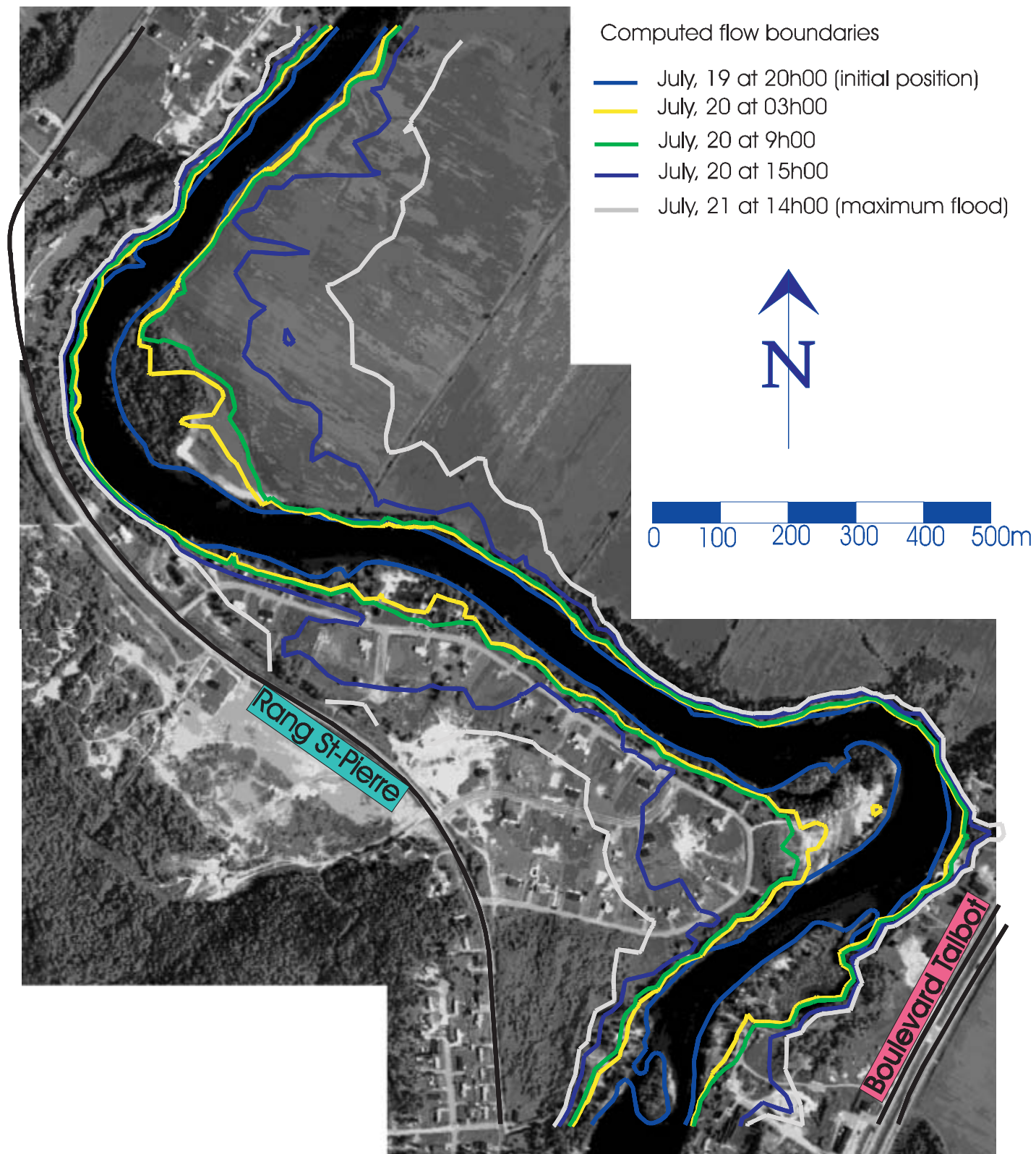


Fig. 15. Saguenay flood: plan view of flood progression.

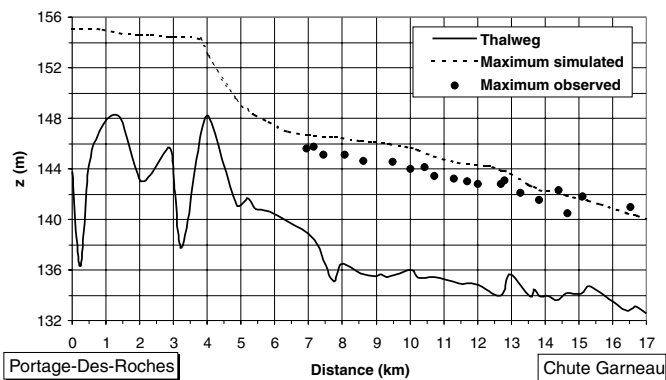


Fig. 16. Saguenay flood: comparison between observed and computed maximum water level values.

References

1. CHOW V.T. (1959). Open-channel hydraulics. McGraw-Hill Civil Engineering Series.
2. FENNEMA R.J. and CHAUDHRY M.H. (1990). Explicit method for 2-D transient free-surface flows. *J. Hydr. Engrg, ASCE*, 116(8), 1013-1033.
3. GALLAND J.C., GOUTAL N. and HERVOUET J.M. (1991). TELEMAC: A new numerical model for solving shallow water equations. *Advances in Water Resources*, 14, 138-148.
4. HENICHE M., SECRETAN Y., BOUDREAU P. and LECLERC M. (2000) A two-dimensional finite element drying-wetting shallow water model for rivers and estuaries. *Advances in Water Resources*, 23, 359-372.
5. HENICHE M., SECRETAN Y. and LECLERC M. (2001). Efficient ILU preconditioning and inexact-Newton-GMRES to solve the 2D steady shallow water equations. *Communications in Numerical Methods in Engineering*, 17, 69-75.
6. INRS-EAU (1997) Simulation hydrodynamique et bilan sédimentaire des rivières Chicoutimi et des Ha! Ha! suite aux crues exceptionnelles de juillet 1996. Technical report R487, INRS-Eau, Université du Québec.
7. KHAN A.A. (2000) Modeling flow over an initially dry bed. *J. Hydr. Research*, 38(5), 383-388.
8. JANSEN PH., VAN BENDEGOM L., VAN DEN BERG J., DE VRIES M., ZANEN A. (1979). Principles of rivers engineering. The non tidal alluvial river. Pitman-London.
9. LAFLEUR J. (1997) Comparaison de deux approches pour la modélisation des microhabitats. M.Sc.report, INRS-Eau, Université du Québec.
10. LECLERC M., HENICHE M., SECRETAN Y. and OUARDA T. (2000). Travaux d'atténuation des risques de crue à l'eau libre de la rivière Montmorency dans le secteur des Îlets-phase 2. Technical report R555, INRS-Eau, Université du Québec, march.
11. LECLERC M., MARION J., HENICHE M., OUARDA T. and SECRETAN Y. (1997). Prediction des dommages résidentiels d'inondation en fonction de l'hydraulicité des rivières Chicoutimi et Aux Sables et du lac Kénogami. Technical report R511, INRS-Eau, Université du Québec, october.
12. LECLERC M., DUMAS G., BELLEMARE J.F. and DHATT G. (1990). A finite element model of estuarine and river flows. *Advances in Water Resources*, 4, 158-168.
13. MORIN, G., PAQUET, P. and SOCHANSKI W. (1995). Le Modèle de simulation de quantité et de qualité CEQUEAU, Manuel de Références, Technical report 433, INRS-Eau, Université du Québec.
14. RODI W. (1984) Turbulence models and their application in hydraulics. State-of-the-art paper, IAHR-AIRH.
15. SECRETAN Y. and LECLERC M. (1998). MODELEUR: a 2D hydrodynamic GIS and simulation software. In the Proceedings of the Third International Conference on Hydroinformatics. Edited by Vladan Babovic & Lars Christian Larsen. Copenhagen, Denmark, 24-26 August, 425-432.
16. ZHANG H., LONG N.D., HASSANZADEH Y. and KAHAWITA R. (1992). A 1-D numerical model applied to dam-break flows on dry beds. *J. Hydr. Research*, 30(2), 211-224.

Notations

The following symbols are used in this paper:

Physical symbols

c	: celerity of shallow water waves;
f_c	: Coriolis force;
g	: gravitational acceleration;
h	: water surface level;
H	: depth;
n	: Manning friction coefficient;
p	: porosity;
$q(q_x, q_y)$: specific discharge vector;
Q	: discharge;
t	: time variable;
$u(u, v)$: horizontal flow velocity components;
$x(x, y)$: Cartesian coordinates;
z_b	: bed topography;
β	: damping coefficient for dry area;
$\tau^b(\tau_x^b, \tau_y^b)$: bottom stresses;
$\tau^s(\tau_x^s, \tau_y^s)$: surface stresses;
ρ	: water density;

FEM and mathematical symbols

$n(n_x, n_y)$: outward unit normal;
Δt	: time step;
Γ	: boundary of computational domain;
Ω	: computational domain;
grad	: gradient operator;
div	: divergence operator;
\otimes	: tensorial product;
[.]	: matrix;
<.>	: row vector;
{.}	: column vector;
.	: absolute value.

Superscripts

b : bottom;
in : inflow;
out : outflow;
s : surface;

Subscripts

c : closed boundary or computed;
e : element;
m : measured;
max : maximum;
min : minimum;
n : normal component;
o : open boundary;
t : tangential component.